



## Discovering low-permittivity materials: Evolutionary search for MgAl<sub>2</sub>O<sub>4</sub> polymorphs

Congwei Xie, Qingfeng Zeng, Artem R. Oganov, and Dong Dong

Citation: [Applied Physics Letters](#) **105**, 022907 (2014); doi: 10.1063/1.4890464

View online: <http://dx.doi.org/10.1063/1.4890464>

View Table of Contents: <http://scitation.aip.org/content/aip/journal/apl/105/2?ver=pdfcov>

Published by the [AIP Publishing](#)

---

### Articles you may be interested in

[First-principle calculation and assignment for vibrational spectra of Ba\(Mg<sub>1/3</sub>Nb<sub>2/3</sub>\)O<sub>3</sub> microwave dielectric ceramic](#)

[J. Appl. Phys.](#) **115**, 114103 (2014); 10.1063/1.4868226

[Melting of -Al<sub>2</sub>O<sub>3</sub> and vitrification of the undercooled alumina liquid: Ab initio vibrational calculations and their thermodynamic implications](#)

[J. Chem. Phys.](#) **138**, 064507 (2013); 10.1063/1.4790612

[Visible photoluminescence from MgAl<sub>2</sub>O<sub>4</sub> spinel with cation disorder and oxygen vacancy](#)

[J. Appl. Phys.](#) **112**, 103523 (2012); 10.1063/1.4767228

[Ab initio many-body study of the electronic and optical properties of MgAl<sub>2</sub>O<sub>4</sub> spinel](#)

[J. Appl. Phys.](#) **111**, 043516 (2012); 10.1063/1.3686727

[Effect of Mg<sup>2+</sup> content on the dielectric properties of Ba<sub>0.65</sub> x Sr<sub>0.35</sub> Mg x TiO<sub>3</sub> ceramics](#)

[J. Appl. Phys.](#) **106**, 014107 (2009); 10.1063/1.3159876

---

The logo for Applied Physics Letters (AIP) is displayed in a white font on an orange background. The letters 'AIP' are large and bold, followed by a vertical bar and the words 'Applied Physics Letters' in a smaller font.

**AIP** | Applied Physics  
Letters

is pleased to announce **Reuben Collins**  
as its new Editor-in-Chief



# Discovering low-permittivity materials: Evolutionary search for MgAl<sub>2</sub>O<sub>4</sub> polymorphs

Congwei Xie,<sup>1,a)</sup> Qingfeng Zeng,<sup>1,b)</sup> Artem R. Oganov,<sup>2,3,4</sup> and Dong Dong<sup>1</sup>

<sup>1</sup>Science and Technology on Thermostructural Composite Materials Laboratory, International Center for Materials Discovery, School of Materials Science and Engineering, Northwestern Polytechnical University, Xi'an, Shaanxi 710072, People's Republic of China

<sup>2</sup>International Center for Materials Discovery, School of Materials Science and Engineering, Northwestern Polytechnical University, Xi'an, Shaanxi 710072, People's Republic of China

<sup>3</sup>Department of Geosciences, Center for Materials by Design, and Institute for Advanced Computational Science, State University of New York, Stony Brook, New York 11794-2100, USA

<sup>4</sup>Moscow Institute of Physics and Technology, Dolgoprudny, Moscow Region 141700, Russia

(Received 31 December 2013; accepted 22 June 2014; published online 16 July 2014)

Low-permittivity ceramics for use as microwave band window materials must have good mechanical and optical characteristics. Unfortunately, most known ceramics are opaque to microwaves because of their high dielectric permittivity. Here, we present an effective theoretical method that may be helpful in the development of innovative low-permittivity materials. Using the material's permittivity as a global optimization function, we performed a crystal structure search for MgAl<sub>2</sub>O<sub>4</sub> using an *ab initio* evolutionary algorithm implemented in the USPEX code. We identified four predicted MgAl<sub>2</sub>O<sub>4</sub> polymorphs ( $P\bar{4}m2$ ,  $P\bar{4}2m$ ,  $Cc$ , and  $Pc$ ) that had lower permittivities than MgAl<sub>2</sub>O<sub>4</sub> spinel ( $Fd\bar{3}m$ ). Our results indicate that the density is not the only factor that affects permittivity. Further analysis of permittivity from the viewpoint of the underlying structures shows that reduced permittivity can be effectively achieved by reducing the cation coordination number. This insight will help in the discovery of materials with minimum permittivity values based on simple crystal-chemical analysis. © 2014 AIP Publishing LLC. [<http://dx.doi.org/10.1063/1.4890464>]

MgAl<sub>2</sub>O<sub>4</sub> spinel ( $Fd\bar{3}m$ ) is one of the most important transparent ceramics, because it allows most electromagnetic waves that are incident upon it to be transmitted, with little of the incident energy being reflected or absorbed.<sup>1–5</sup> This functional ceramic material also has some other excellent properties, including high corrosion resistance, high melting point, good abrasion resistance, and good chemical stability.<sup>6–9</sup> As a result, MgAl<sub>2</sub>O<sub>4</sub> spinel is considered to be an excellent transparent material for optical and electronic component applications in devices.<sup>10–12</sup> However, MgAl<sub>2</sub>O<sub>4</sub> spinel is a typical transparent ceramic in that it is readily transparent to infrared wavelengths, while it remains opaque to microwaves.<sup>13</sup> The main reason for this is that the transmittance  $T$ , which represents the proportion of electromagnetic wave transmitted by the material, varies with the electromagnetic wave frequency. The transmittance  $T$  is calculated from

$$T = 1 - R - A. \quad (1)$$

The reflectivity  $R$ , which describes the proportion of the electromagnetic wave that is reflected, can be calculated from the material's permittivity  $\epsilon$  and the angle of incidence  $\theta$  using the Fresnel equation, which, for a non-magnetic material in air under normal incidence, reduces to

$$R = \left(1 - \frac{2}{\sqrt{\epsilon} + 1}\right)^2. \quad (2)$$

The absorptivity  $A$ , which is the proportion of the electromagnetic wave that is absorbed by the material, is approximately equal to zero for ideal materials in non-peculiar frequency bands. Eqs. (1) and (2) demonstrate that as the permittivity  $\epsilon$  increases, then  $R$  also increases, and thus,  $T$  becomes smaller.

MgAl<sub>2</sub>O<sub>4</sub> spinel has much higher permittivity in the microwave band (8.38,<sup>14</sup> 8.42<sup>15</sup>) than in the infrared band (2.96,<sup>15</sup> 2.98<sup>5</sup>). Therefore, it is an intriguing prospect to make MgAl<sub>2</sub>O<sub>4</sub> spinel transparent in microwave band by reducing its permittivity. Two effective paths can be used: the design of a porous structure or the design of a composite with a low- $\kappa$  substance.<sup>16</sup> However, we have also considered another idea: that of replacing the MgAl<sub>2</sub>O<sub>4</sub> spinel structure with a different structure that has the same chemical composition but lower permittivity. A number of methods have been developed to discover crystal structures that offer minima or maxima of certain properties<sup>17</sup> when only their chemical compositions are initially provided. The most widely used of these methods is the *ab initio* evolutionary algorithm implemented in the USPEX<sup>18–20</sup> code, which has been applied to the optimization of various material properties other than the energy.<sup>21,22</sup> In particular, we recently demonstrated optimization of the material permittivity and related functions<sup>23</sup> using this method. In this paper, using MgAl<sub>2</sub>O<sub>4</sub> as an example, we show how to use the method to explore potential MgAl<sub>2</sub>O<sub>4</sub> polymorphs with lower permittivities than MgAl<sub>2</sub>O<sub>4</sub> spinel.

The permittivity is a tensorial quantity that is closely related to the crystal structure, the electronic structure, and the lattice dynamics. We use the orientationally-averaged

<sup>a)</sup>Electronic mail: xiecw1021@mail.nwpu.edu.cn

<sup>b)</sup>Electronic mail: qfzeng@nwpu.edu.cn

static permittivity  $\bar{\epsilon}_0$  as the fitness function, because most dielectrics are used in their polycrystalline form. The fitness value  $\bar{\epsilon}_0$  can be obtained from  $\bar{\epsilon}_0 = (\epsilon_0^{xx} + \epsilon_0^{yy} + \epsilon_0^{zz})/3$ , where  $\epsilon_0^{xx}$ ,  $\epsilon_0^{yy}$ , and  $\epsilon_0^{zz}$  are the diagonal components of the static dielectric tensor. We have searched for the lowest-permittivity structure at 0 GPa with up to 14 atoms (2 formula unit) in the unit cell. For every candidate structure generated by USPEX, we used *ab initio* structure relaxations based on density functional theory<sup>24</sup> (DFT) within the functional PBEsol,<sup>25</sup> a version of the generalized gradient approximation<sup>26</sup> (GGA) adapted for solids, as implemented in the VASP code.<sup>27</sup> The all-electron projector-augmented wave (PAW) method,<sup>28</sup> with a plane-wave kinetic energy cutoff of 900 eV and k-point meshes with reciprocal-space resolution of  $2\pi \times 0.06 \text{ \AA}^{-1}$ , was used. These settings enable excellent convergences for the energy differences, stress tensors, and structural parameters. Then, denser k-point meshes with reciprocal-space resolution of  $2\pi \times 0.04 \text{ \AA}^{-1}$  were used for the calculations of the properties. Density functional perturbation theory<sup>29</sup> (DFPT) was applied to investigate the dielectric properties of each relaxed candidate structure.

A typical *ab initio* run for  $\text{MgAl}_2\text{O}_4$  is as shown in Fig. 1. The figure depicts the permittivity and enthalpy values of the explored structures. We also plotted the most stable spinel phase (denoted by the leftmost point in Fig. 1) at ambient pressure for reference. The lowest permittivity (3.01) was indicated by a layered structure ( $P\bar{1}$  phase). However, this structure is rather unrealistic because of its high enthalpy (0.51 eV/atom greater than the spinel phase). The  $\text{MgAl}_2\text{O}_4$  polymorphs ( $P\bar{4}m2$ ,  $P\bar{4}2m$ ,  $Cc$ , and  $Pc$ ) with their low permittivity and enthalpy values (within 0.20 eV/atom of the ground-state structure) are much more plausible. The permittivities of these materials are 19% (6.64), 30% (5.72), 27% (5.96), and 35% (5.35) lower than that of the spinel phase (8.19), respectively. We have computed phonon dispersion curves<sup>30</sup> and the elastic constants<sup>31</sup> for these materials and found the four structures to be both dynamically and mechanically stable—see Fig. S1 and Table SI in the supplementary material.<sup>32</sup> In other words, the predicted structures can exist as real materials

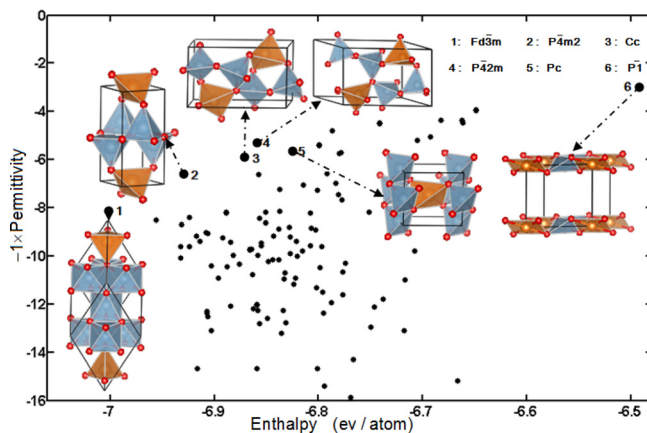


FIG. 1. Typical *ab initio* run for  $\text{MgAl}_2\text{O}_4$ , depicting the permittivity and enthalpy values (eV/atom) of the structures produced by USPEX. The inset sub-graphs show the crystal structures of the  $\text{MgAl}_2\text{O}_4$  polymorphs as follows: 1— $Fd\bar{3}m$  phase; 2— $P\bar{4}m2$  phase; 3— $P\bar{4}2m$  phase; 4— $Cc$  phase; 5— $Pc$  phase; 6— $P\bar{1}$  phase. The red spheres denote O atoms, the grey spheres denote Al atoms, and the brown spheres denote Mg atoms.

and may be suitable for applications as microwave-transparent phases. For example, one could fabricate these phases by epitaxial growth on a suitably chosen substrate in the future. Geometry details of the predicted phases are listed in Table I. The spinel phase details were also listed for reference. The crystal structures of the  $\text{MgAl}_2\text{O}_4$  polymorphs were illustrated by the inserted sub graphs (visualized using VESTA<sup>33</sup>) in Fig. 1. The spinel phase contains magnesium atoms in the tetrahedral coordination and aluminum atoms in the octahedral coordination. The  $P\bar{4}m2$  phase has magnesium atoms in the tetrahedral coordination and aluminum atoms in the 5-coordinate positions. The other three phases,  $P\bar{4}2m$ ,  $Cc$ , and  $Pc$ , have both magnesium and aluminum atoms in the tetrahedral coordination.

We then studied the factors that make the predicted structures have relatively low permittivity. We first built the relationship between the permittivity and density (as shown in Fig. 2). The figure shows that the  $P\bar{4}2m$  phase is 1% denser than the  $P\bar{4}m2$ , but its permittivity is 14% lower; the  $Cc$  and  $Pc$  phases have nearly the same density, while their permittivities differ by 10%. For different substances, such as the  $\text{MgAl}_2\text{O}_4$  polymorphs that are reported here, density is not the only factor that affects their permittivity.

We can write (Ref. 29):

$$\Delta\epsilon = \bar{\epsilon}_0 - \bar{\epsilon}_\infty = \frac{4\pi}{V} \sum_m \frac{S_m}{\omega_m^2}. \quad (3)$$

Here,  $\bar{\epsilon}_\infty$  is the electronic permittivity,  $V$  is the volume of the primitive unit cell, and  $\omega_m$  and  $S_m$  are the frequency and

TABLE I. Geometrical details of the  $\text{MgAl}_2\text{O}_4$  polymorphs discovered using USPEX.

Compound	Space group (No.)	Lattice constants (Å)	Atom position (Wyckoff position)
Cubic $\text{MgAl}_2\text{O}_4$	$Fd\bar{3}m$ (227)	$a = 8.111$ $a = 8.083^{38}$	Mg(8a) (0, 0, 0)
			Al(16d) (0.625, 0.625, 0.625)
			O(32e) (0.389, 0.389, 0.389)
Tetragonal $\text{MgAl}_2\text{O}_4$	$P\bar{4}m2$ (115)	$a = 3.460$ $c = 6.990$	Mg(1b) (0.500, 0.500, 0)
			Al(2g) (0, 0.500, 0.391)
			O1(1c) (0.500, 0.500, 0.500)
Tetragonal $\text{MgAl}_2\text{O}_4$	$P\bar{4}2m$ (111)	$a = 4.196$ $c = 4.719$	Mg(1a) (0, 0, 0)
			Al(2f) (0.500, 0, 0.500)
			O(4n) (0.242, 0.758, 0.709)
Monoclinic $\text{MgAl}_2\text{O}_4$	$Cc$ (9)	$a = 4.811$ $b = 8.948$ $b = 8.548$ $\beta = 110.122$	Mg(4a) (0.726, 0.194, 0.873)
			Al1(4a) (1.368, 0.937, 0.619)
			Al2(4a) (0.765, 0.122, 0.500)
			O1(4a) (1.462, 0.790, 0.505)
			O2(4a) (0.590, 0.900, 0.151)
			O3(4a) (1.437, 0.132, 0.322)
Monoclinic $\text{MgAl}_2\text{O}_4$	$Pc$ (7)	$a = 5.034$ $b = 5.321$ $b = 8.199$ $\beta = 128.204$	Mg(2a) (0.892, 0.169, 0.792)
			Al1(2a) (0.402, 0.937, 0.619)
			Al2(2a) (0.649, 0.323, 1.045)
			O1(2a) (0.564, 0.647, 1.025)
			O2(2a) (0.014, 0.274, 1.063)
			O3(2a) (0.710, 0.827, 0.758)
			O4(2a) (0.324, 0.138, 0.835)

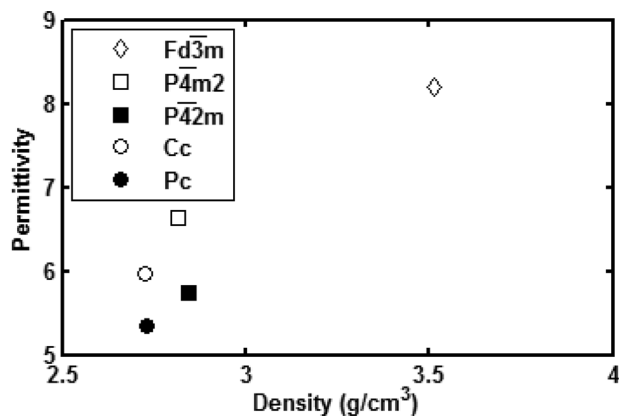


FIG. 2. Relationships between permittivity and density ( $\text{g/cm}^3$ ) for the  $Fd\bar{3}m$ ,  $P\bar{4}m2$ ,  $P\bar{4}2m$ ,  $Cc$ , and  $Pc$  phases.

the oscillator strength of the  $m$ th mode, respectively. We can see that the permittivity is also affected by  $\omega_m$  and  $S_m$ , which differ from structure to structure. Therefore, it seems reasonable to explain the differences in permittivity from a structure properties viewpoint. We preferentially selected coordination polyhedra that were formed by cations and their nearest anions as structural units (SUs), not merely because they are both simple and common but also because they can quantify permittivity well.<sup>34</sup>

The relationship between permittivity and the characteristic quantities ( $Z$  and  $C^{-1}$ ) that is used to describe coordination polyhedron is as follows (Ref. 34):

$$\Delta\varepsilon = \frac{4\pi Z^2}{\bar{V}C}. \quad (4)$$

The characteristic dynamical charge  $Z$  is defined by  $Z^2 = (\sum_{\kappa} Z_{\kappa}^2)/N$ , where  $Z_{\kappa}$  represents the atomic Born effective charges of the atom  $\kappa$  and  $N$  the number of SUs. According to Eqs. (3) and (4), the characteristic force constant  $C$  is defined using  $C^{-1} = ((\sum_m S_m/\omega_m^2)/Z^2)/N$ . Averaged volume  $\bar{V}$  is simply  $V/N$ . Larger values of  $Z$  and  $C^{-1}$  will, therefore, lead to higher permittivities. The spinel phase has two  $\text{MgO}_4$  and four  $\text{AlO}_6$  SUs in the primitive cell. The  $P\bar{4}m2$  phase has one  $\text{MgO}_4$  and two  $\text{AlO}_5$  SUs in the primitive cell. The  $P\bar{4}2m$ ,  $Cc$ , and  $Pc$  phases all have two  $\text{MgO}_4$  and four  $\text{AlO}_4$  SUs in the primitive cell. We have

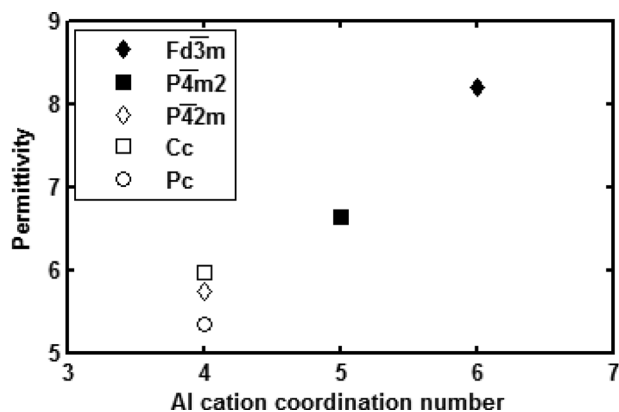


FIG. 3. Average static permittivity  $\bar{\varepsilon}_0$  computed for the  $Fd\bar{3}m$ ,  $P\bar{4}m2$ ,  $P\bar{4}2m$ ,  $Cc$ , and  $Pc$  phases in relation to the Al cation coordination number in each case.

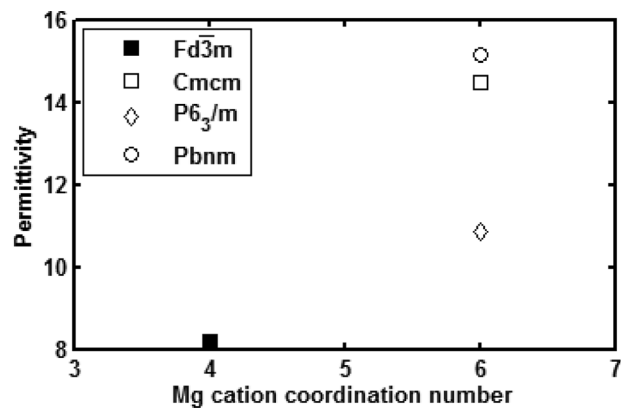


FIG. 4. Average static permittivity  $\bar{\varepsilon}_0$  computed for the  $Fd\bar{3}m$ ,  $Cmcm$ ,  $P6_3/m$ , and  $Pbnm$  phases in relation to the Mg cation coordination number in each case.

assumed the  $\text{MgO}_4$  SU plays an equal role in all these structures because it has an unchangeable coordination environment among all these polymorphs. Using the five structures, we construct the relationship between the permittivity and the coordination polyhedra (represented by the coordination number of Al cations), as shown in Fig. 3. It is clear that permittivity increased with the coordination number of the Al cations. We have also calculated the permittivity of three other experimentally reported high-pressure  $\text{MgAl}_2\text{O}_4$  polymorphs ( $Cmcm$ ,  $Pbnm$ , and  $P6_3/m$ ) that contain both magnesium and aluminum atoms in the octahedral coordination.<sup>35</sup> As shown in Fig. 4, an increased Mg coordination number can also lead to the enhancement of the permittivity. The theoretical values of  $\bar{V}$ ,  $Z$ , and  $C^{-1}$  for the eight  $\text{MgAl}_2\text{O}_4$  polymorphs are listed in Table II. The tendencies for these values to vary with coordination polyhedra are shown in Fig. 5. It is likely that the increased coordination number will cause  $\bar{V}$  to decrease, while  $Z$  increases as the coordination number increase. Most importantly,  $C^{-1}$  increase occurs on increasing coordination number.

We performed an in-depth analysis of the contribution of each IR-active mode to the permittivity—see Table SII in the supplementary material.<sup>32</sup> To do this, we investigated the origins of the different  $C^{-1}$  values by looking at the atomic vibrations for modes that make a large contribution to the

TABLE II. Cation coordination number, average static permittivity  $\bar{\varepsilon}_0$ , average electronic permittivity  $\bar{\varepsilon}_{\infty}$ , and average properties of  $(\text{MgO}_m + 2\text{AlO}_n)$  SUs—volume  $\bar{V}$  ( $\text{\AA}^3$ ), characteristic dynamical charge  $Z$ , and reciprocal force constant  $C^{-1}$ . The subscript  $m$  is the coordination number of the Mg cation, and the subscript  $n$  is the coordination number of the Al cation.

Phase	Coordination number		$\bar{\varepsilon}_{\infty}$	$\bar{\varepsilon}_0$	$\bar{V}$ ( $\text{\AA}^3$ )	$Z$	$C^{-1}$
	$\text{Mg}^{2+}$	$\text{Al}^{3+}$					
$Fd\bar{3}m$	4	6	3.10	8.19	22.40	3.36	0.80
$P\bar{4}m2$	4	5	2.83	6.64	27.97	3.15	0.85
$P\bar{4}2m$	4	4	2.86	5.73	27.69	3.04	0.68
$Cc$	4	4	2.73	5.96	28.90	3.09	0.78
$Pc$	4	4	2.73	5.35	28.85	3.06	0.64
$Cmcm$	6	6	3.30	14.46	20.05	3.53	1.43
$P6_3/m$	6	6	3.45	10.84	20.94	3.54	0.98
$Pbnm$	6	6	3.31	15.13	20.12	3.51	1.54

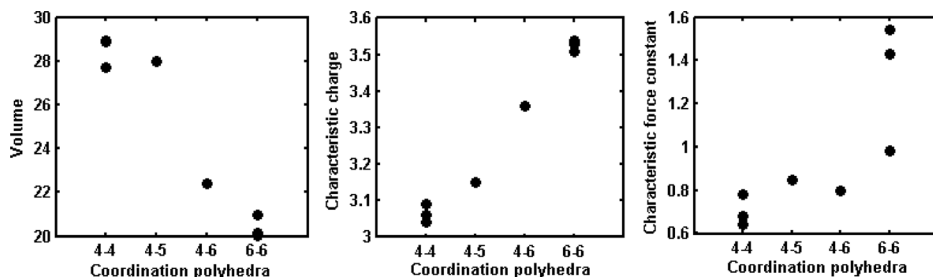


FIG. 5. Atomic properties ( $\bar{V}$  ( $\text{\AA}^3$ ),  $Z$ , and  $C^{-1}$ ) computed for the  $Fd\bar{3}m$ ,  $P\bar{4}m2$ ,  $P\bar{4}2m$ ,  $Cc$ ,  $Pc$ ,  $Cmcm$ ,  $P6_3/m$ , and  $Pbnm$  phases in relation to their coordination polyhedra. The value of the abscissa is represented by  $m-n$ , where  $m$  is the Mg cation coordination number and  $n$  the Al cation coordination number.

permittivity. For the  $Fd\bar{3}m$  phase, the  $T_{1u}$  vibrational mode at  $472\text{ cm}^{-1}$  makes the largest contribution to the permittivity. The atomic vibrations of the octahedral  $\text{AlO}_6$  SU under this mode are shown in Fig. 6(a). The central Al atom moves to one side, while the six O atoms almost travel in the opposite direction. The nature of the atomic vibrations will introduce a large distortion to the  $\text{AlO}_6$  SU, and thus, a large  $C^{-1}$  is produced because of the high oscillator strength  $S_m$ . For the  $P\bar{4}m2$  phase, appreciable distortion of the square pyramid  $\text{AlO}_5$  SU can be observed at  $525\text{ cm}^{-1}$  ( $E$  mode). Fig. 6(b) shows the atomic vibrations for this  $E$  mode in detail: the O atom located at the top of the square pyramid is motionless, the other four O atoms and the Al atom have exactly opposite movements. This distortion of the square pyramid  $\text{AlO}_5$  SU can also produce a large  $C^{-1}$ . It seems that the large distortion is difficult to induce in tetrahedral  $\text{AlO}_4$  SU.<sup>36</sup> As shown in Fig. 6(c), all four O atoms simply rock around the central Al atoms.

Overall, the  $\text{MgAl}_2\text{O}_4$  polymorphs that have high coordination numbers have weaker bonds and are easily deformed (higher  $C^{-1}$ ), are denser (lower  $\bar{V}$ ) and more ionic (larger  $Z$ ), which leads to the enhancement of permittivity according to Eq. (4). This insight will help us to discover materials with minimum/maximum values of permittivity based on simple crystal-chemical analysis. This analysis also justifies the use of empirical polarizable force fields (e.g., those including the shell model<sup>37</sup>) for the discovery of low-/high- $\kappa$  materials, because these force fields are capable of producing reasonable relaxed geometries, polarizabilities, force constants, and effective Born charges.

In this paper, using evolutionary crystal structure prediction, we have explored energetically permissible structures for  $\text{MgAl}_2\text{O}_4$  that have low permittivity. We found four  $\text{MgAl}_2\text{O}_4$  polymorphs ( $P\bar{4}m2$ ,  $P\bar{4}2m$ ,  $Cc$ , and  $Pc$ ), with permittivities that are 19%, 30%, 27%, and 35% lower than the known spinel phase, respectively. Our results indicate that, even for

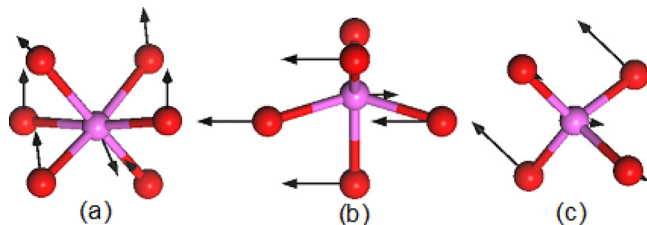


FIG. 6. Atomic vibrations of  $\text{AlO}_x$  ( $x=4, 5$ , and  $6$ ) SUs for modes that make large contributions to the permittivity: (a)  $\text{AlO}_6$  SU in the  $Fd\bar{3}m$  phase for the  $T_{1u}$  mode at  $472\text{ cm}^{-1}$ ; (b)  $\text{AlO}_5$  SU in the  $P\bar{4}m2$  phase for the  $E$  mode at  $525\text{ cm}^{-1}$ ; and (c)  $\text{AlO}_4$  SU in the  $P\bar{4}2m$  phase for the  $E$  mode at  $326\text{ cm}^{-1}$ . The red spheres denote O atoms, and the pink spheres denote Al atoms.

structures with the same chemical composition, the density of each material is not the only factor that affects its permittivity. Further analysis of the permittivity has been conducted from a crystal structure viewpoint. We first used two characteristic quantities ( $Z$  and  $C^{-1}$ ) to describe coordination polyhedra of the  $\text{MgAl}_2\text{O}_4$  polymorphs and associated them with the permittivity. Then, we obtained their exact values from first-principles calculations. Our results show that structures with high coordination numbers have weaker bonds (higher  $C^{-1}$ ) are more ionic (larger  $Z$ ), and likely to be denser (lower  $\bar{V}$ ), all these factors leading to higher permittivity. Finally, by analyzing atomic vibrations of the  $\text{AlO}_x$  ( $x=4, 5$ , and  $6$ ) SUs, we found that the high coordination number coordination polyhedra are easily deformed, and thus, a large  $C^{-1}$  is produced.

This work was supported by the Basic Research Foundation of NWPU (No. JCY20130114), the Natural Science Foundation of China (Nos. 51372203 and 51332004), the Foreign Talents Introduction and Academic Exchange Program of China (No. B08040), the National Science Foundation (EAR-1114313, DMR-1231586), DARPA (Grants No. W31P4Q1310005 and No. W31P4Q1210008), CRDF Global (UKE2-7034-KV-11), the Government (No. 14.A12.31.0003) and the Ministry of Education and Science of Russian Federation (Project No. 8512). The authors also acknowledge the High Performance Computing Center of NWPU for the allocation of computing time on their machines.

<sup>1</sup>M. Shimada, T. Endo, T. Saito, and T. Sato, *Mater. Lett.* **28**, 413 (1996).

<sup>2</sup>C. Wang and Z. Zhao, *Scr. Mater.* **61**, 193 (2009).

<sup>3</sup>I. Reimanis and H.-J. Kleebe, *J. Am. Ceram. Soc.* **92**, 1472 (2009).

<sup>4</sup>S. Meir, S. Kalabukhov, N. Froumin, M. P. Dariel, and N. Frage, *J. Am. Ceram. Soc.* **92**, 358 (2009).

<sup>5</sup>Q. Zeng, L. Zhang, X. Zhang, Q. Chen, Z. Feng, Y. Cai, L. Cheng, and Z. Weng, *Phys. Lett. A* **375**, 3521 (2011).

<sup>6</sup>I. Ganesh, *Int. Mater. Rev.* **58**, 63 (2013).

<sup>7</sup>W.-C. Tsai, Y.-H. Liou, and Y.-C. Liou, *Mater. Sci. Eng. B* **177**, 1133 (2012).

<sup>8</sup>C.-J. Ting and H.-Y. Lu, *Acta Mater.* **47**, 817 (1999).

<sup>9</sup>A. Goldstein, A. Goldenberg, Y. Yeshurun, and M. Hefetz, *J. Am. Ceram. Soc.* **91**, 4141 (2008).

<sup>10</sup>E. Strassburger, *J. Eur. Ceram. Soc.* **29**, 267 (2009), special Issue on Transparent Ceramics.

<sup>11</sup>A. Krell, J. Klimke, and T. Hutzler, *J. Eur. Ceram. Soc.* **29**, 275 (2009), special Issue on Transparent Ceramics.

<sup>12</sup>G. Wei, *J. Phys. D: Appl. Phys.* **38**, 3057 (2005).

<sup>13</sup>K. Surendran, P. Bijumon, P. Mohanan, and M. Sebastian, *Appl. Phys. A* **81**, 823 (2005).

<sup>14</sup>P. Fu, Y. Xu, W. Lu, W. Lei, X. Wang, and X. Ruan, *Int. J. Appl. Ceram. Technol.* **39**, 2481 (2013).

<sup>15</sup>C. Wang and P. Zanzucchi, *J. Electrochem. Soc.* **118**, 586 (1971).

<sup>16</sup>M. Rubat du Merac, I. E. Reimanis, C. Smith, H.-J. Kleebe, and M. M. Miller, *Int. J. Appl. Ceram. Technol.* **10**, E33 (2013).

<sup>17</sup>*Modern methods of crystal structure prediction*, edited by A. R. Oganov (Wiley-VCH, Berlin, 2011).

- <sup>18</sup>A. R. Oganov and C. W. Glass, *J. Chem. Phys.* **124**, 244704 (2006).
- <sup>19</sup>C. W. Glass, A. R. Oganov, and N. Hansen, *Comput. Phys. Commun.* **175**, 713 (2006).
- <sup>20</sup>A. O. Lyakhov, A. R. Oganov, and M. Valle, *Comput. Phys. Commun.* **181**, 1623 (2010).
- <sup>21</sup>A. O. Lyakhov and A. R. Oganov, *Phys. Rev. B* **84**, 092103 (2011).
- <sup>22</sup>Q. Zhu, A. R. Oganov, M. A. Salvadó, P. Pertierra, and A. O. Lyakhov, *Phys. Rev. B* **83**, 193410 (2011).
- <sup>23</sup>Q. Zeng, A. R. Oganov, A. O. Lyakhov, C. Xie, X. Zhang, J. Zhang, Q. Zhu, B. Wei, I. Grigorenko, L. Zhang, and L. Cheng, *Acta Crystallogr., Sect. C* **70**, 76 (2014).
- <sup>24</sup>P. Hohenberg and W. Kohn, *Phys. Rev.* **136**, B864 (1964).
- <sup>25</sup>J. P. Perdew, A. Ruzsinszky, G. I. Csonka, O. A. Vydrov, G. E. Scuseria, L. A. Constantin, X. Zhou, and K. Burke, *Phys. Rev. Lett.* **100**, 136406 (2008).
- <sup>26</sup>J. P. Perdew, K. Burke, and M. Ernzerhof, *Phys. Rev. Lett.* **77**, 3865 (1996).
- <sup>27</sup>G. Kresse and J. Furthmüller, *Phys. Rev. B* **54**, 11169 (1996).
- <sup>28</sup>P. E. Blöchl, *Phys. Rev. B* **50**, 17953 (1994).
- <sup>29</sup>S. Baroni, S. de Gironcoli, A. Dal Corso, and P. Giannozzi, *Rev. Mod. Phys.* **73**, 515 (2001).
- <sup>30</sup>A. Togo, F. Oba, and I. Tanaka, *Phys. Rev. B* **78**, 134106 (2008).
- <sup>31</sup>R. A. Cowley, *Phys. Rev. B* **13**, 4877 (1976).
- <sup>32</sup>See supplementary material at <http://dx.doi.org/10.1063/1.4890464> for studying the dynamical, mechanical, and vibrational properties of the MgAl<sub>2</sub>O<sub>4</sub> polymorphs.
- <sup>33</sup>K. Momma and F. Izumi, *J. Appl. Crystallogr.* **44**, 1272 (2011).
- <sup>34</sup>G.-M. Rignanese, F. Detraux, X. Gonze, A. Bongiorno, and A. Pasquarello, *Phys. Rev. Lett.* **89**, 117601 (2002).
- <sup>35</sup>S. Ono, J. Brodholt, and G. Price, *Phys. Chem. Miner.* **35**, 381 (2008).
- <sup>36</sup>C. Xie, Q. Zeng, D. Dong, S. Gao, Y. Cai, and A. R. Oganov, *Phys. Lett. A* **378**, 1867 (2014).
- <sup>37</sup>B. G. Dick and A. W. Overhauser, *Phys. Rev.* **112**, 90 (1958).
- <sup>38</sup>H. Sawada, *Mater. Res. Bull.* **30**, 341 (1995).